41st Danubia-Adria Symposium Advances in Experimental Mechanics
September 23-26, 2025, Kragujevac, Serbia

DOI: 10.46793/41DAS2025.071R

AUTOMATION OF CONSTITUTIVE MODEL PARAMETER IDENTIFICATION

Dragan RAKIĆ[1], Slobodan RADOVANOVIĆ[2], Miroslav ŽIVKOVIĆ[3]

[1] 0000-0001-5152-5788, Faculty of Engineering University of Kragujevac, Sestre Janjić 6, Kragujevac, Serbia, E-mail: drakic@kg.ac.rs;

[2] 0000-0002-8437-9016, Water Institute "Jaroslav Černi" Belgrade, Jaroslava Černog 80, Belgrade, Serbia, E-mail: slobodan.radovanovic@jcerni.rs;

[3] 0000-0002-0752-6289, Faculty of Engineering University of Kragujevac, Sestre Janjić 6, Kragujevac, Serbia, E-mail: zile@kg.ac.rs;

1. Introduction

For reliable stability analysis of geotechnical structures, accurate calibration of constitutive model parameters is essential. These parameters govern the simulated material response under load, and any uncertainty can lead to significant deviations in predicted behavior.

Conventional parameter determination relies on experimental testing of soil samples, whereby stress–strain measurements are used to infer individual model parameters according to their constitutive definitions. However, this manual fitting process is complex and time-consuming, particularly for soils, which exhibit highly nonlinear behavior.

To address these challenges, we propose an automated parameter identification procedure for constitutive models. The methodology is developed for the Modified Cam-Clay model (MCC), a widely adopted framework for simulating the mechanical response of soft clays and normally consolidated soils.

The first part of this paper presents the theoretical foundations and the implicit stress integration algorithm for the MCC model, implemented within the PAK [1] finite element software. For automated identification [2], the same integration scheme is translated into Python and applied at the level of single integration point. This point-wise approach is justified for homogeneous stress states, such as those encountered in standard laboratory tests (e.g., oedometer and triaxial tests).

In the second part of the paper, we describe the parameter identification program, which interfaces with the Python integration routine to perform optimization against experimental data. Finally, the developed identification algorithm is verified through a comparison of parameter estimates obtained from the PAK-based finite element implementation and those produced by the automated procedure.

2. Theoretical basis of the Modified Cam-Clay constitutive model

The yield surface of the MCC model [3] in space $q-\sigma_m$ is shown in Fig. 1.

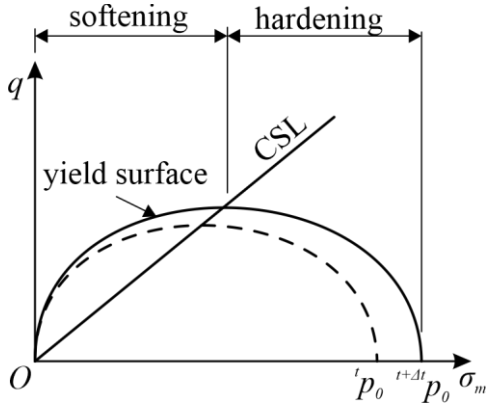

Fig. 1. Modified Cam-Clay model yield surface

The yield surface equation of MCC model is a function of stress states and has the form

$$f = q^2 - M^2\sigma_m\left(p_o - \sigma_m\right) \tag{1}$$

In equation (1), the quantity M represents the material parameter, while the quantities q and σ_m are the stress deviator

$$q = \sqrt{3J_{2D}} \tag{2}$$

and mean stress

$$\sigma_m = \sigma_x + \sigma_y + \sigma_z \tag{3}$$

The quantity p_0 defines the size of the yield surface according to the expression

$$ {}^{t+\Delta t}p_o = {}^{t}p_o \exp\left(\frac{-\Delta e_m^P}{{}^{t+\Delta t}b_V}\right) \tag{4} $$

where Δe_m^p is the increment of mean plastic strain, while

$$ {}^{t+\Delta t}b_V = \frac{k_s}{3\left(1+{}^{t+\Delta t}e\right)} \tag{5} $$

$$ k_s = \lambda - \kappa \tag{6} $$

The current porosity, in expression (5) is calculated according to

$$ {}^{t+\Delta t}e = \left(1+{}^{0}e\right)\mathrm{e}^{{}^{t+\Delta t}e_V} - 1 \tag{7} $$

where ${}^{0}e$ is the initial porosity of the material, while ${}^{t+\Delta t}e_V$ is the current volumetric strain.

The elasticity modulus of MCC constitutive model depends on the strain history and is defined according to

$$ {}^{t+\Delta t}E = 3\left(1-2\nu\right){}^{t+\Delta t}K \tag{8} $$

where is it

$$ {}^{t+\Delta t}K = \frac{1+{}^{t+\Delta t}e}{\kappa}\,{}^{t+\Delta t}\sigma_m \tag{9} $$

The algorithm for implicit stress integration [4] of the MCC model, using the previously shown theoretical foundations, implemented in the PAK program and in the Python code at the integration point level, is shown in Table 1.

Table 1. Stress integration algorithm for MCC model

Known at the beginning of time step: ${}^{t+\Delta t}\mathbf{e}$, ${}^{t}\mathbf{e}$, ${}^{t}\boldsymbol{\sigma}$, ${}^{t}\mathbf{e}^{p}$

A. Trial (elastic) solution:

$d\boldsymbol{\sigma} = \mathbf{C}^E d\mathbf{e}^E = \mathbf{C}^E\left({}^{t+\Delta t}\mathbf{e} - {}^{t}\mathbf{e}\right)$, ${}^{t+\Delta t}\boldsymbol{\sigma} = {}^{t}\boldsymbol{\sigma} + d\boldsymbol{\sigma}$

Calculation of stress invariants:

I_1, J_{2D}

$q = \sqrt{3J_{2D}}$,

Yield surface:

$k_s = \lambda - \kappa$, $e = \left(1+{}^{0}e\right)\exp\left(e_V\right) - 1$

$b_V = \frac{k_s}{3\left(1+e\right)}$, $p_o = {}^{t}p_o \exp\left(\frac{\Delta e_m^P}{b_V}\right)$

$f = g = q^2 - M^2\sigma_m\left(p_o - \sigma_m\right)$

B. Checking yield condition:

IF ($f < 0$) goto **E**

IF ($f \geq 0$) continue

Yield area check ${}^{t+\Delta t}\sigma_m^E \leftrightarrow \frac{1}{2}{}^{t}p_0$

$$ \frac{\partial f}{\partial \boldsymbol{\sigma}} = \frac{\partial f}{\partial q}\frac{\partial q}{\partial \boldsymbol{\sigma}} + \frac{\partial f}{\partial I_1}\frac{\partial I_1}{\partial \boldsymbol{\sigma}} + \frac{\partial f}{\partial {}^{t}p_0}\frac{\partial {}^{t}p_0}{\partial \boldsymbol{\sigma}} $$

$$ d\lambda = \frac{\frac{\partial f}{\partial \boldsymbol{\sigma}}^{\mathrm{T}}\mathbf{C}^E d\mathbf{e}}{\frac{\partial f}{\partial \boldsymbol{\sigma}}^{\mathrm{T}}\mathbf{C}^E\frac{\partial f}{\partial \boldsymbol{\sigma}} + {}^{t}p_0\frac{1+{}^{t+\Delta t}e}{k_s}\cdot\frac{\partial f}{\partial {}^{t}p_0}\mathbf{I}\frac{\partial g}{\partial \boldsymbol{\sigma}}} $$

C. Correction of dλ (local iterations):

$d\mathbf{e}^P = d\lambda\frac{\partial g}{\partial \boldsymbol{\sigma}}$, $d\mathbf{e}^E = d\mathbf{e} - d\mathbf{e}^P$

$d\boldsymbol{\sigma} = \mathbf{C}^E d\mathbf{e}^E$, ${}^{t+\Delta t}\boldsymbol{\sigma} = {}^{t}\boldsymbol{\sigma} + d\boldsymbol{\sigma}$

Calculation of new stress invariants:

I_1, J_{2D}

Yield condition:

${}^{t+\Delta t}e = \left(1+{}^{0}e\right)\exp\left({}^{t+\Delta t}e_V\right) - 1$,

${}^{t+\Delta t}b_V = \frac{k_s}{3\left(1+{}^{t+\Delta t}e\right)}$,

${}^{t+\Delta t}p_o = {}^{t}p_o \exp\left(\frac{\Delta e_m^P}{{}^{t+\Delta t}b_V}\right)$,

${}^{t+\Delta t}E = 3\left(1-2\nu\right){}^{t+\Delta t}K$

$f = q^2 - M^2\sigma_m\left(p_o - \sigma_m\right)$

D. IF ($ABS(f) \geq TOL$) goto **C** with new $d\lambda$:

${}^{t+\Delta t}\mathbf{e}^P = {}^{t}\mathbf{e}^P + d\mathbf{e}^P$

E. End: ${}^{t+\Delta t}\boldsymbol{\sigma}$, ${}^{t+\Delta t}\mathbf{e}^P$

3. Parameter Calibration of the Constitutive Model

The identification procedure is performed at the level of a single integration point, where homogeneous stress and strain states can be assumed. This localized approach isolates material behavior from boundary and geometric effects, making it directly comparable to standard laboratory tests.

As inputs, the algorithm accepts stress-strain histories obtained experimentally. Depending on the test setup, either the applied loading (stress-controlled) or the measured deformation (strain-controlled) path can be imposed. The numerical simulation replicates these paths exactly, ensuring that the same increments of loading or deformation are evaluated.

A scalar objective function quantifies the discrepancy between experimental and simulated responses. Commonly, this function is based on an error norm, such as the mean absolute or squared difference, possibly supplemented by weighting schemes that emphasize critical segments of the loading path (e.g., peak stress). Penalty terms enforce physical consistency by discouraging nonphysical behaviors, such as softening under

monotonic load or unbounded state variables. Simulations yielding unstable or divergent results incur large penalties.

Each model parameter is confined to a predefined interval reflecting prior geotechnical knowledge. These bounds prevent exploration of unrealistic regimes, enhance numerical stability, and accelerate convergence by reducing the viable search space.

A hybrid, two-stage optimization strategy ensures both global exploration and local precision:

- Global Search: An evolutionary algorithm (e.g., differential evolution) samples the parameter space broadly, locating low-error regions and mitigating entrapment in local minima.

- Local Refinement: A gradient-based or quasi-Newton method (e.g., L-BFGS-B) is initialized from the best global solution to achieve fine-scale convergence, leveraging derivative information for efficient adjustments.

This combined approach balances robustness and accuracy, yielding a parameter set that faithfully reproduces the experimental loading path.

4. Validation

Parameter identification was performed using oedometer test results, selected for their nearly homogeneous stress state within the specimen, which makes them particularly suitable for the proposed single-point calibration procedure. Initial lower and upper bounds for each constitutive parameter were set based on physical plausibility and geotechnical knowledge, ensuring that the optimization remained within realistic regimes.

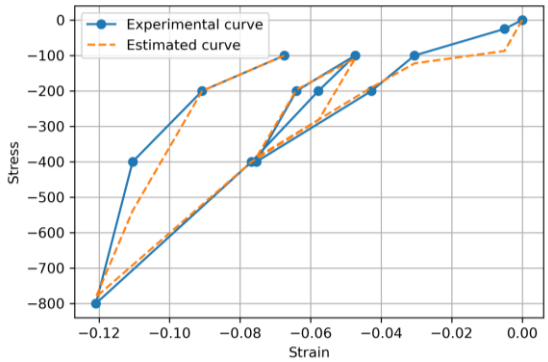

Fig. 2. Oedometer test 1: Experimental and estimated dependence

The resulting experimental stress-strain paths and the simulated model responses are overlaid in Fig. 2-Fig. 4, demonstrating close agreement across elastic, yield, and hardening phases. Quantitative assessment via maximum relative error and coefficient of determination (R^2) confirms that the calibrated model reproduces laboratory observations within acceptable tolerance, thereby validating the robustness and fidelity of the automated identification algorithm.

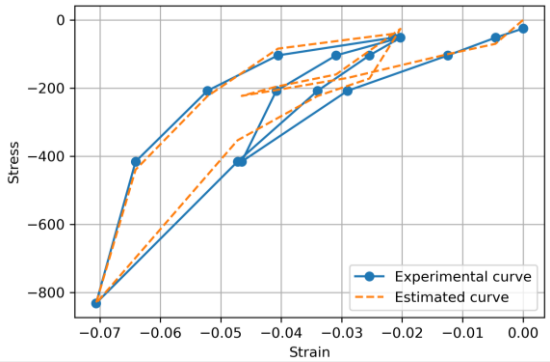

Fig. 3. Oedometer test 2: Experimental and estimated dependence

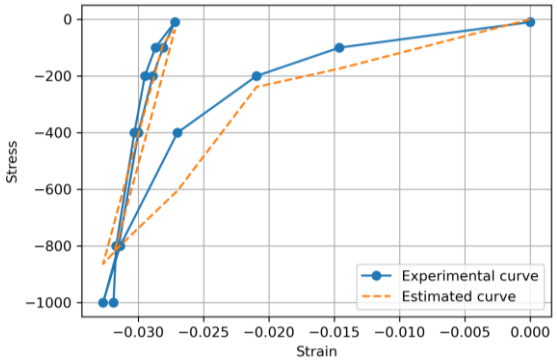

Fig. 4 Oedometer test 3: Experimental and estimated dependence

After completing parameter identification, a numerical simulation of the same oedometer test was executed in the PAK finite element program under identical boundary and loading conditions.

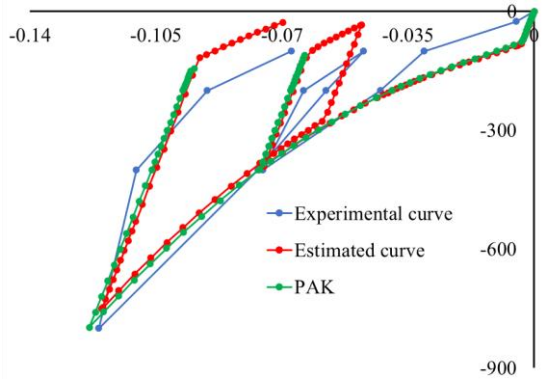

Fig. 5. Results of numerical simulation of oedometer test 1

The calibrated parameters were then applied in the Python-based integration routine over the same number of increments as in PAK. The results of

these simulations, alongside the experimental curves, are presented in Fig. 5-Fig. 7, further substantiating the equivalence of the standalone Python algorithm and the PAK implementation.

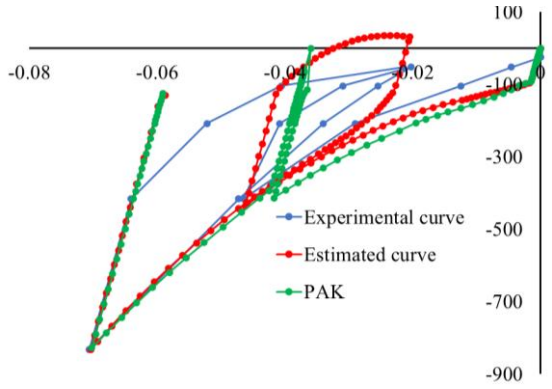

Fig. 6. Results of numerical simulation of oedometer test 2

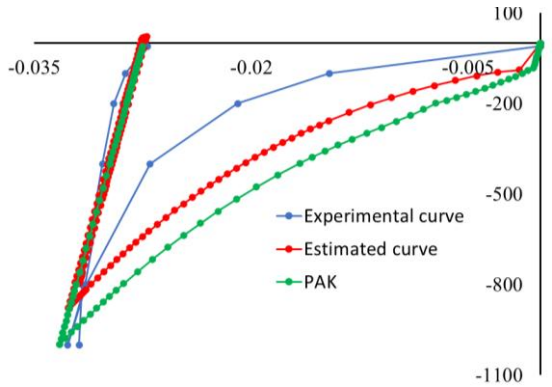

Fig. 7. Results of numerical simulation of oedometer test 3

The results indicate that the responses predicted by the automated identification closely match the experimental data, confirming the procedure's accuracy. Discrepancies between the Python-based and PAK simulations can be attributed to methodological differences: the Python routine performs point-wise stress integration without element mesh interactions, whereas the PAK implementation relies on full finite element discretization.

5. Conclusions

The conducted study demonstrates that the automated parameter identification procedure provides a reliable and efficient means of calibrating the constitutive model. By relying on oedometer test data, the method ensured stable convergence and consistent results within realistic geotechnical ranges.

The obtained simulations show that the approach is capable of capturing the full stress–strain behavior, including elasticity, yield and subsequent hardening. This consistency across both the standalone Python routine and the PAK program highlights the robustness and transferability of the calibration procedure.

While discrepancies between implementations were observed, these stem primarily from the inherent differences between point-wise stress integration and finite element discretization. Importantly, such deviations do not undermine the predictive capability of the method but instead underline the complementary strengths of simplified integration routines and full numerical simulations.

Overall, the proposed procedure offers a validated framework for parameter calibration that balances computational efficiency with accuracy. Its integration into broader numerical workflows can support more reliable geotechnical analyses and provide a solid foundation for future extensions to more complex soil constitutive models.

Acknowledgments

This research was supported by the Science Fund of the Republic of Serbia, #GRANT No 7475, Prediction of damage evolution in engineering structures - PROMINENT and by the Ministry of Science, Technological Development and Innovation, Republic of Serbia, Agreement No. 451-03-137/2025-03/200107.

References

[1] Živković, M., Kojić, M., Slavković, R., Grujović, N., Rakić, D., Dunić, V. PAK-S, Program for FE Structural Analysis of Solids and Structures, University of Kragujevac, Faculty of Engineering, Kragujevac, 2019.
[2] Furukawa, T., Sugata, T., Yoshimura, S., Hoffman, M. An automated system for simulation and parameter identification of inelastic constitutive models, Computer Methods in Applied Mechanics and Engineering, 2002, 191(21-22), 2235-2260.
[3] Borja, R. I., Lee, S. R, Cam-clay plasticity, part 1: implicit integration of elasto-plastic, Computer Methods in Applied Mechanics and Engineering, 1990, 78(1), 49-72.
[4] Bathe K.J, Finite element procedures, USA: Massachusetts Institute of Technology, 1996.